Inorg. Chem. **2003**, *42*, 633–640

Syntheses, Structures, and Electronic Interactions of Dicyanamide/Tricyanomethanide-Bridged Binuclear Organometallic Complexes

Li-Yi Zhang,[†] Lin-Xi Shi,[†] and Zhong-Ning Chen*[,†,‡,§]

State Key Laboratory of Structural Chemistry, Fujian Institute of Research on the Structure of Matter, Chinese Academy of Sciences, Fuzhou, Fujian 350002, China, State Key Laboratory of Organometallic Chemistry, Shanghai Institute of Organic Chemistry, Chinese Academy of Sciences, Shanghai 200032, China, and State Key Laboratory of Coordination Chemistry, Nanjing University, Nanjing 210093, China

Received July 17, 2002

Dicyanamide-bound mononuclear compounds $Cp(dppe)FeN(CN)_2$ (**3**) and $Cp(PPh_3)_2RuN(CN)_2$ (**4**) were isolated in high yields by the reactions of Cp(dppe)FeCl (**1**) and $Cp(PPh_3)_2RuCl$ (**2**), respectively, with excess sodium dicyanamide. Compounds **3** and **4** are excellent precursors for the design of dicyanamide-bridged binuclear complexes $[\{Cp(dppe)Fe\}_2N(CN)_2](SbF_6)$ (**5**) and $[\{Cp(PPh_3)_2Ru\}_2N(CN)_2](SbF_6)$ (**6**) by the incorporation with **1** and **2**, respectively. Controlling oxidation of **5** with ferrocenium hexafluorophosphate afforded the mixed-valence compound $[\{Cp(dppe)Fe\}_2N(CN)_2](PF_6)_2$ (**5a**) which exhibits a broad absorption band in the near-infrared region (centered at 1500 nm, $\epsilon = 750$ cm^{-1} M^{-1}) due to the intervalence charge transfer of Robin and Day class II mixed-valence system. Tricyanomethanide-bound mononuclear compounds $Cp(dppe)FeC(CN)_3$ (**7**) and $Cp(PPh_3)_2RuC(CN)_3$ (**8**) were prepared by the same methods as **3** and **4** using potassium tricyanomethanide as the starting material instead. The tricyanomethanide-bridged binuclear complexes $[\{Cp(dppe)Fe\}_2C(CN)_3](CF_3SO_3)$ (**9**) and $[\{Cp(PPh_3)_2Ru\}_2C(CN)_3](SbF_6)$ (**10**) were prepared by the reactions between **7** and **1** and between **8** and **2**, respectively. Cyclic voltammograms of the dicyanamide/tricyanomethanide-bridged binuclear complexes showed stepwise reversible one-electron oxidation waves with the potential separation of the two redox couples in the range 0.14–0.25 V, indicating the demonstrably electronic communication is operative between the organometallic components through a dicyanamide/tricyanomethanide spacer with metal···metal distances more than 7.8 Å. Furthermore, the electronic coupling transmitted by the tricyanomethanide is appreciably greater than that by the dicyanamide. The complexes **3**–**10** were characterized by elemental analysis, IR, UV–vis, ^{1}H and ^{31}P NMR, and ES-MS. The crystal structures of **3** and **5**–**9** were determined by X-ray crystallography.

Introduction

Transition metal complexes that exhibit electronic delocalization are of current interest because of their potential application as molecular wires which are essential for the assembly of nanoscale electronic devices.[1−6] The linear assembly molecules that consist of an organic unsaturated conjugated spacer linking two redox-active metal termini could permit electron flow to occur along the molecular backbone. The mediated electronic effect between the redox-active termini through an organic spacer is usually evaluated by electrochemical measurements. When different redox states are stably present at both ends of the spacer, an odd electron-containing species or mixed-valence compound can be generated by an electrochemical or/and chemical redox

* Corresponding author. E-mail: czn@ms.fjirsm.ac.cn. Fax: +86-591-379-2346.
† Fujian Institute of Research on the Structure of Matter.
‡ State Key Laboratory of Organometallic Chemistry.
§ State Key Laboratory of Coordination Chemistry.

(1) Paul, F.; Lapinte, C. *Coord. Chem. Rev.* **1998**, *178*−*180*, 431.
(2) Ziessel, R.; Hissler, M.; El-ghayoury, A.; Harriman, A. *Coord. Chem. Rev.* **1998**, *178*−*180*, 1251.
(3) Patoux, C.; Launay, J.-P.; Beley, M.; Chodorowski-Kimmes, S.; Collin, J.-P.; James, S.; Sauvage, J.-P. *J. Am. Chem. Soc.* **1998**, *120*, 3717.
(4) Astruc, D. *Acc. Chem. Res.* **1997**, *30*, 383.
(5) Hradsky, A.; Bildstein, B.; Schuler, N.; Schottenberger, H.; Jaitner, P.; Ongania, K.-H.; Wurst, K.; Launay, J.-P. *Organometallics* **1997**, *16*, 392.
(6) (a) Barigelletti, F.; Flamigni, L. *Chem. Soc. Rev.* **2000**, *29*, 1. (b) Sato, M.; Shintate, H.; Kawata, Y.; Sekino, M.; Katada, M.; Kawata, S. *Organometallics* **1994**, *13*, 1956.

10.1021/ic025879t CCC: $25.00
Published on Web 12/20/2002

method, and a wealth of decisive information about through-bridge electron transfer can be recognized by UV−vis−NIR spectrometry.[7−20]

Dicyanamide ($N(CN)_2^-$)[21,22] and tricyanomethanide ($C(CN)_3^-$)[23,24] are versatile for the design of polymeric metal architectures by self-assembly. They behave frequently as μ- or/and μ_3-bridges linking two or three metal centers to produce 1D, 2D, or 3D extended aggregates. The bridging array M−N≡C−N−C≡N−M′/M−N≡C−C(CN)−C≡N−M′ is nonlinear owing to the sp^2 hybridization of the middle nitrogen/carbon atom with M···M′ separation more than 7.5 Å. However, it is essential to detect the capability of dicyanamide/tricyanomethanide as a spacer to mediate electronic effect between two redox-active organometallic centers.[25,26] Thus, a series of dicyanamide/tricyanomethanide-containing mono- and binuclear complexes were prepared and characterized by spectroscopic measurements and X-ray crystallography. Herein are described the preparation and characterization of the dicyanamide/tricyanomethanide-containing mono- or dinuclear organometallic complexes together with a mixed-valence binuclear complex [{Cp(dppe)Fe}$_2$N(CN)$_2$](PF$_6$)$_2$ (**5a**).

Experimental Section

Material and Reagents. All operations were performed in an atmosphere of dry argon by using Schlenk and vacuum techniques. Solvents were dried by standard methods and distilled prior to use. The reagents sodium dicyanamide ($NaN(CN)_2$), potassium tricyanomethanide ($KC(CN)_3$), thallium cyclopentadienide, dicyclopentadiene, triphenylphosphine (PPh_3), 1,2-bis(diphenylphosphino)-ethane (dppe), potassium triflate (KCF_3SO_3), and sodium hexafluoroantimonate ($NaSbF_6$) were purchased from commercial sources (Acros, Fluka, and Aldrich Chemicals Co.). The organometallic compounds Cp(dppe)FeCl (**1**)[27] and Cp(PPh_3)$_2$RuCl (**2**)[28] were prepared by the reported procedures.

Cp(dppe)FeN(CN)$_2$ (3). Compound **1** (1.0 mmol, 545.0 mg) and $NaN(CN)_2$ (3.0 mmol, 267.0 mg) were added into 20 mL of methanol which was stirred at room temperature for 2 h to give a deep red solution. The solvent was removed in vacuo, and the residue was dissolved in 5 mL of dichloromethane. After taken by filtration, the filtrate was purified by chromatography using aluminum oxide column. Elution with dichloromethane gave the pure product. Yield: 75%. Layering petroleum ether onto the 1,2-dichloroethane solution afforded the product as crystals. Anal. Calcd for $C_{33}H_{29}FeN_3P_2\cdot0.5C_2H_4Cl_2$: C, 64.32; H, 4.92; N, 6.62. Found: C, 64.68; H, 4.72; N, 6.44. IR spectrum (KBr, cm^{-1}): ν 2266 (m, $N(CN)_2$), 2224 (w, $N(CN)_2$), 2158 (s, $N(CN)_2$). ^{1}H NMR spectrum ($CDCl_3$): δ 7.77−7.26 (m, 20H, C_6H_5), 4.14 (s, 5H, C_5H_5), 3.73 (s, 2H, $C_2H_4Cl_2$), 2.28 (d, 4H, $P(CH_2)_2P$). ^{31}P NMR spectrum ($CDCl_3$): δ 99.4 (s). UV−vis (λ_{max}/nm (ϵ, cm^{-1} M^{-1})): 235 (58000), 315 (3900), 383 (1400).

Cp(PPh$_3$)$_2$RuN(CN)$_2$ (4). To a dichloromethane (20 mL) solution of Cp(PPh_3)$_2$RuCl (0.20 mmol, 145.2 mg) was added a methanol (5 mL) solution of $NaN(CN)_2$ (0.50 mmol, 44.5 mg) with the color change from orange into pale yellow. After the solution was stirred at room temperature for 4 h, the solvents were evaporated in vacuo to leave a residue which was dissolved in 3 mL of dichloromethane. After taken by filtration, the filtrate was layered with petroleum ether to give pale yellow crystals of the product. Yield: 88%. Anal. Calcd for $C_{43}H_{35}N_3P_2Ru$: C, 68.25; H, 4.66; N, 5.55. Found: C, 68.44; H, 4.25; N, 5.36. IR spectrum (KBr, cm^{-1}): ν 2270 (s, $N(CN)_2$), 2229 (m, $N(CN)_2$), 2164 (s, $N(CN)_2$). ^{1}H NMR spectrum ($CDCl_3$): δ 7.31−7.15(m, 30H, C_6H_5), 4.20 (s, 5H, C_5H_5). ^{31}P NMR spectrum ($CDCl_3$): δ 43.3 (s). UV−vis (λ_{max}/nm (ϵ, cm^{-1} M^{-1})): 231 (17000), 351 (1100).

[{Cp(dppe)Fe}$_2$N(CN)$_2$](SbF$_6$) (5). To a methanol (5 mL) solution of **1** (0.10 mmol, 55.5 mg) was added first a methanol (5 mL) solution of **3** (0.10 mmol, 58.5 mg), and then sodium hexafluoroantimonate (0.11 mmol, 28.5 mg). The solution color changed rapidly into deep red. After the solution was stirred at room temperature for 2 h, the methanol was evaporated in vacuo to leave a residue which was dissolved in 2 mL of dichloromethane.

(7) Keyes, T. E.; Forster, R. J.; Jayaweera, P. M.; Coates, C. G.; McGarvey, J. J.; Vos, J. G. *Inorg. Chem.* **1998**, *37*, 5925.
(8) (a) Barrado, G.; Carriedo, G. A.; Diaz-Valenzuela, C.; Riera, V. *Inorg. Chem.* **1991**, *30*, 4416. (b) Coe, B, J.; Meyer, T. J.; White, P. S. *Inorg. Chem.* **1995**, *34*, 3600. (c) Richardson, G. N.; Brand, U.; Vahrenkamp, H. *Inrog. Chem.* **1999**, *38*, 3070. (d) Zhu, N.; Vahrenkamp, H. *Chem. Ber.* **1997**, *130*, 1241.
(9) (a) Xu, D.; Hong, B. *Angew. Chem., Int. Ed.* **2000**, *39*, 1826. (b) Ortega, J. V.; Hong, B.; Ghosal, S.; Hemminger, J. C.; Breedlove, B.; Kubiak, C. P. *Inorg. Chem.* **1999**, *38*, 5102.
(10) Coe, B. J.; Meyer, T. J.; White, P. S. *Inorg. Chem.* **1995**, *34*, 593.
(11) (a) Pfennig, B. W.; Lockard, J. V.; Cohen, J. L.; Watson, D. F.; Ho, D. M.; Bocarsly, A. B. *Inorg. Chem.* **1999**, *38*, 2941. (b) Pfennig, B. W.; Cohen, J. L.; Sosnowski, I.; Novotny, N. M.; Ho, D. M. *Inorg. Chem.* **1999**, *38*, 606.
(12) (a) Brady, M.; Weng, W.; Zhou, Y.; Seyler, J. W.; Amoroso, A. J.; Arif, A. M.; Böhme, M.; Frenking, G.; Gladysz, J. A. *J. Am. Chem. Soc.* **1997**, *119*, 775. (b) Paul, F.; Meyer, W. E.; Toupet, L.; Jiao, H.; Gladysz, J. A.; Lapinte, C. *J. Am. Chem. Soc.* **2000**, *122*, 9405. (c) Narvor, N. L.; Toupet, L.; Lapinte, C. *J. Am. Chem. Soc.* **1995**, *117*, 7129. (d) Kheradmandan, S.; Heinze, K.; Schmalle, H.; Berke, H. *Angew. Chem., Int. Ed.*. **1999**, *38*, 2270.
(13) Wong, K.-T.; Lehn, J.-M.; Peng, S.-M.; Lee, G.-H. *Chem. Commun.* **2000**, 2259.
(14) (a) Ren, T.; Zou, G.; Alvarez, J. C. *Chem. Commun.* **2000**, 1197. (b) Bear, J. L.; Han, B.; Wu, Z.; Van Caemelbecke, E.; Kadish, K. M. *Inrog. Chem.* **2001**, *40*, 2275.
(15) (a) Bruce, M. I.; Hall, B. C.; Kelly, B. D.; Low, P. J.; Skelton, B. W.; White, A. H. *J. Chem. Soc., Dalton Trans.* **1999**, 3719. (b) Bruce, M. I.; Hinterding, P.; Tiekink, E. R. T. *J. Organomet. Chem.* **1993**, *450*, 209. (c) Bruce, M. I.; Low, P. J.; Costuas, K.; Halet, J.-F.; Best, S. P.; Heath, G. A. *J. Am. Chem. Soc.* **2000**, *122*, 1949.
(16) Dembinski, R.; Bartik, T.; Bartik, B.; Jaeger, M.; Gladysz, J. A. *J. Am. Chem. Soc.* **2000**, *122*, 810.
(17) (a) Lebreton, C.; Touchard, D.; Pichon, L. L.; Daridor, A.; Toupet, L.; Dixneuf, P. H. *Inorg. Chim. Acta* **1998**, *272*, 188. (b) Lavastre, O.; Plass, J.; Bachmann, P.; Guesmi, S.; Moinet, C.; Dixneuf, P. H. *Organometallics* **1997**, *16*, 184.
(18) (a) Jones, N. D.; Wolf, M. O.; Giaquinta, D. M. *Organometallics* **1997**, *16*, 1352. (b) Hore, L.-A.; McAdam, C. J.; Kerr, J. L.; Duffy, N. W.; Robinson, B. H.; Simpson, J. *Organometallics* **2000**, *19*, 5039.
(19) (a) Creutz, C. C. *Prog. Inorg. Chem.* **1983**, *30*, 1. (b) Dog, Y.; Hupp, J. T. *Inorg. Chem.* **1992**, *31*, 3170.
(20) Nihei, M.; Nankawa, T.; Kurihara, M.; Nishihara, H. *Angew. Chem., Int. Ed.* **1999**, *38*, 1098.
(21) (a) Jensen, P.; Price, D. J.; Batten, S. R.; Moubaraki, B.; Murray, K. S. *Chem. Eur. J.* **2000**, *6*, 3186. (b) van der Werff, P. M.; Batten, S. R.; Jensen, P.; Moubaraki, B.; Murray, K. S. *Inorg. Chem.* **2001**, *40*, 1718. (c) Batten, S. R.; Jensen, P.; Moubaraki, B.; Murray, K. S. *Chem. Commun.* **2000**, 2331.
(22) (a) Marshall, S. R.; Incarvito, C. D.; Manson, J. L.; Rheingold, A. L.; Miller, J. S. *Inorg. Chem.* **2000**, *39*, 1969. (b) Manson, J. L.; Lee, D. W.; Rheingold, A. L.; Miller, J. S. *Inorg. Chem.* **1998**, *37*, 5966.
(23) (a) Batten, S. R.; Hoskins, B. F.; Robson, R. *Chem. Commun.* **1991**, 445. (b) Batten, S. R.; Hoskins, B. F.; Moubaraki, B.; Murray, K. S.; Robson, R. *J. Chem. Soc., Dalton Trans.* **1999**, 2977.
(24) Manson, J. L.; Ressouche, E.; Miller, J. S. *Inorg. Chem.* **2000**, *39*, 1135.
(25) Kuang, S.-M.; Fanwick, P. E.; Walton, R. A. *Inorg. Chem.* **2002**, *41*, 147.
(26) Miyasaka, H.; Clerac, R.; Campos-Fernandez, C. S.; Dunbar, K. R. *Inorg. Chem.* **2001**, *40*, 1663.
(27) Mays, M. J.; Sears, P. L. *J. Chem. Soc., Dalton Trans.* **1973**, 1873.
(28) Bruce, M. I.; Windsor, N. J. *Aust. J. Chem.* **1977**, *30*, 1601.

After taken by filtration, the product was crystallized by layering petroleum ether onto the dichloromethane solution. Yield: 80%. Anal. Calcd for $C_{64}H_{58}N_3F_6P_4Fe_2Sb\cdot CH_2Cl_2\cdot 2CH_3OH$: C, 54.03; H, 4.60; N, 2.82. Found: C, 53.93; H, 4.28; N, 2.58. ES-MS (*m*/*z*): 1339 ([{Cp(dppe)Fe}$_2$N(CN)$_2$(SbF$_6$)$^+$]), 1104 ([{Cp(dppe)Fe}$_2$N(CN)$_2$]$^+$), 561 ([Cp(dppe)FeNCN]$^+$), 519 ([Cp(dppe)Fe]$^+$). IR spectrum (KBr, cm^{-1}): ν 2299 (m, N(CN)$_2$), 2208 (s, N(CN)$_2$), 658 (s, SbF$_6$). ^{1}H NMR spectrum (CDCl$_3$): δ 7.63−7.15 (m, 40H, C$_6H_5$), 4.19 (s, 10H, C$_5$H$_5$), 2.25 (s, 8H, P(CH_2)$_2$P). UV−vis (λ_{max}/nm (ϵ, cm^{-1} M^{-1})): 234 (52000), 316 (39000), 479 (800).

[{Cp(dppe)Fe}$_2$N(CN)$_2$](PF$_6$)$_2$ (5a). To a dichloromethane (10 mL) solution of [{Cp(dppe)Fe}$_2$N(CN)$_2$](PF$_6$) (0.10 mmol, 125 mg) was added ferrocenium hexafluorophosphate (0.10 mmol, 33.1 mg) with stirring at room temperature for 2 h. The solution was then concentrated, leaving 2 mL of the volume. Diffusion of diethyl either gave a precipitate which was washed with diethyl ether three times and redissolved in 10 mL of dichloromethane with stirring for 2 h. The solution was concentrated again and diffused with diethyl ether to precipitate the product which was disposed repeatedly for three times by the same procedure. Crystallization in dichloromethane−petroleum gave the pure product. Yield: 51%. Anal. Calcd for $C_{64}H_{58}F_{12}N_3P_6Fe_2\cdot 0.5CH_2Cl_2$: C, 53.91; H, 4.14; N, 2.92. Found: C, 53.99; H, 3.77; N, 2.77. IR spectrum (KBr, cm^{-1}): ν 2233 (m, N(CN)$_2$), 2187 (m, N(CN)$_2$), 2087 (m, N(CN)$_2$), 839 (s, PF$_6$). UV−vis−NIR (λ_{max}/nm (ϵ, cm^{-1} M^{-1})): 230 (41000), 317 (4400), 1550 (750).

[{Cp(PPh$_3$)$_2$Ru}$_2$N(CN)$_2$](SbF$_6$) (6). To a dichloromethane (5 mL) solution of **2** (0.10 mmol, 72.6 mg) was added first a dichloromethane (5 mL) solution of **4** (0.1 mmol, 75.7 mg), and then a methanol (2 mL) solution of sodium hexafluoroantimonate (0.11 mmol, 28.5 mg). The solution was stirred at room temperature for 4 h with the solution color changing from orange into earthy yellow. The solvents were removed in vacuo to leave a yellow residue which was dissolved in 3 mL of dichloromethane. After taken by filtration, the filtrate was layered with petroleum ether for crystallization of the product. Yield: 75%. Anal. Calcd for $C_{84}H_{70}N_3F_6P_4Ru_2Sb$: C, 59.94; H, 4.19; N, 2.50. Found: C, 59.78; H, 4.26; N, 2.39. ES-MS (*m*/*z*): 1448 ([{Cp(PPh$_3$)$_2$Ru}$_2$N(CN)$_2$]$^+$), 731 ([Cp(PPh$_3$)$_2$RuNCN]$^+$), 691 ([Cp(PPh$_3$)$_2$Ru]$^+$), 626 ([(PPh$_3$)$_2$Ru]$^+$). IR spectrum (KBr, cm^{-1}): ν 2295 (m, N(CN)$_2$), 2208 (s, N(CN)$_2$), 658 (s, SbF$_6$). ^{1}H NMR spectrum (CDCl$_3$): δ7.29−7.10 (m, 60H, C$_6H_5$), 4.24 (s, 10H, C$_5$H$_5$). ^{31}P NMR spectrum (CDCl$_3$): δ 41.4 (s). UV−vis (λ_{max}/nm (ϵ, cm^{-1} M^{-1})): 234 (88000), 321 (6100).

Cp(dppe)FeC(CN)$_3$ (7). To a dichloromethane (15 mL) solution of **1** (0.20 mmol, 111.0 mg) was added a methanol solution of potassium tricyanomethanide (0.40 mmol, 51.6 mg) with rapid color change from deep dark red into red. After the solution was stirred at room temperature for 2 h, the solvents were removed to leave a red residue which was dissolved in 5 mL of dichloromethane. After taken by filtration, the filtrate was chromatographed by an aluminum oxide column, and the red band was collected using dichloromethane−methanol (50:1) as eluate. Yield: 81%. Anal. Calcd for $C_{35}H_{29}FeN_3P_2$: C, 68.98; H, 4.80; N, 6.89. Found: C, 68.48; H, 4.77; N, 6.59. IR spectrum (KBr, cm^{-1}): ν 2168 (s, C(CN)$_3$). ^{1}H NMR spectrum (CDCl$_3$): δ 7.69−7.27 (m, 20H, C$_6H_5$), 4.23 (s, 5H, C$_5$H$_5$), 2.30 (d, 4H, P(CH_2)$_2$P). ^{31}P NMR spectrum (CDCl$_3$): δ 98.7 (s). UV−vis (λ_{max}/nm (ϵ, cm^{-1} M^{-1})): 234 (44000), 319 (3000), 470 (700).

Cp(PPh$_3$)$_2$RuC(CN)$_3$ (8). To a dichloromethane (15 mL) solution of **2** (0.20 mmol, 145.2 mg) was added a methanol (4 mL) solution of potassium tricyanomethanide (0.40 mmol, 51.6 mg). The solution was stirred at room temperature for 4 h accompanied by the color change from orange-red into pale yellow. The solvents were removed in vacuo, and the residue was dissolved in 3 mL of dichloromethane. The product was isolated as a precipitate by layering petroleum ether onto the solution. After taken by filtration, the product was recrystallized in 1,2-dichloroethane−petroleum ether to give yellow crystals. Yield: 88%. Anal. Calcd for $C_{45}H_{35}N_3P_2Ru$: C, 69.22; H, 4.52; N, 5.38. Found: C, 69.72; H, 4.05; N, 5.08. IR spectrum (KBr, cm^{-1}): ν 2175 (s, C(CN)$_3$). ^{1}H NMR spectrum (CDCl$_3$): δ 7.34−7.09 (m, 30H, C$_6H_5$), 4.29 (s, 5H, C$_5$H$_5$). ^{31}P NMR spectrum (CDCl$_3$): δ 42.1 (s). UV−vis (λ_{max}/nm (ϵ, cm^{-1} M^{-1})): 234 (45000), 340 (2700).

[{Cp(dppe)Fe}$_2$C(CN)$_3$](CF$_3$SO$_3$) (9). To a dichloromethane (10 mL) solution of **7** (0.10 mmol, 60.9 mg) was added first a dichloromethane (5 mL) solution of **1** (0.10 mmol, 55.5 mg), and then a methanol (3 mL) solution of potassium trifluoromethanesulfonate (0.12 mmol, 22.6 mg). After the solution was stirred at room temperature for 4 h, the solvents were evaporated in vacuo, and the residue was dissolved in 3 mL of dichloromethane. After taken by filtration, the filtrate was layered with petroleum ether to crystallize the product. Yield: 85%. Anal. Calcd for $C_{67}H_{58}F_3Fe_2N_3O_3P_4S$: C, 62.98; H, 4.57; N, 3.29. Found: C, 63.69; H, 4.27; N, 3.19. ES-MS (*m*/*z*): 1128 ([{Cp(dppe)Fe}$_2$C(CN)$_3$]$^+$), 607 ([Cp(dppe)FeC(CN)$_3$]$^+$), 517 ([Cp(dppe)Fe]$^+$). IR spectrum (KBr, cm^{-1}): ν 2201 (w, C(CN)$_3$), 2179 (s, C(CN)$_3$), 1277 (s, CF$_3$SO$_3$), 1174 (m, CF$_3$SO$_3$), 1032 (m, CF$_3$SO$_3$). ^{1}H NMR spectrum (CDCl$_3$): δ 7.74−7.19 (m, 40H, C$_6H_5$), 4.14 (s, 10H, C$_5$H$_5$), 2.48 (d, 4H, P(CH_2)$_2$P), 2.07 (s, 4H, P(CH_2)$_2$P). ^{31}P NMR spectrum (CDCl$_3$): δ 97.1 (s). UV−vis (λ_{max}/nm (ϵ, cm^{-1} M^{-1})): 230 (65000), 268 (27000), 472 (1000).

[{Cp(PPh$_3$)$_2$Ru}$_2$C(CN)$_3$](SbF$_6$) (10). Compounds **8** (0.10 mmol, 78.1 mg) and **2** (0.10 mmol, 72.6 mg) were put into a 25 mL Schlenk flask and dissolved in 10 mL of dichloromethane with stirring. A methanol (5 mL) solution of sodium hexafluoroantimonate (0.12 mmol, 31.5 mg) was then added, and the solution was stirred at room temperature for 4 h with the color change from orange-red into earthy yellow. The solvents were removed in vacuo to leave a residue which was dissolved in 3 mL of dichloromethane. After filtration, the filtrate was layered with petroleum ether to afford the product as a precipitate which was washed with diethyl ether three times. The product was recrystallized in dichloromethane−petroleum ether. Yield: 81%. Anal. Calcd for $C_{86}H_{70}F_6N_3P_4Ru_2Sb\cdot 0.5CH_2Cl_2$: C, 59.38; H, 4.09; N, 2.40. Found: C, 59.61; H, 3.90; N, 2.72. ES-MS (*m*/*z*): 1470 ([{Cp(PPh$_3$)$_2$Ru}$_2$C(CN)$_3$]$^+$), 691 ([Cp(PPh$_3$)$_2$Ru]$^+$). IR spectrum (KBr, cm^{-1}): ν 2202 (m, C(CN)$_3$), 2185 (s, C(CN)$_3$), 656 (s, SbF$_6$). ^{1}H NMR spectrum (CDCl$_3$): δ 7.47−7.06 (m, 60H, C$_6H_5$), 4.33 (s, 10H, C$_5$H$_5$). ^{31}P NMR spectrum (CDCl$_3$): δ 42.3 (s). UV−vis (λ_{max}/nm (ϵ, cm^{-1} M^{-1})): 234 (88000), 321 (6100).

X-ray Crystallography. Crystals suitable for X-ray diffraction were grown by layering petroleum ether onto the 1,2-dichloroethane solution for **3**$\cdot 1/2C_2H_4Cl_2$ and **8**$\cdot H_2O$, by diffusion of petroleum ether into the dichloromethane−methanol (4:1) solutions for **5**$\cdot CH_2Cl_2\cdot 2CH_3OH$ and **6**$\cdot 2CH_2Cl_2\cdot 1/2CH_3OH\cdot 3/2H_2O$, and by layering hexane onto the dichloromethane solutions for **7** and **9**. Crystallographic parameters and details for data collection and refinement were summarized in Table 1 for **3**$\cdot 1/2CH_2ClCH_2Cl$, **5**$\cdot CH_2Cl_2\cdot 2CH_3OH$, and **6**$\cdot 2CH_2Cl_2\cdot 1/2CH_3OH\cdot 3/2H_2O$ and in Table 2 for **7**, **8**, and **9**. Full crystallographic data are provided in the Supporting Information.

Single crystals sealed in capillaries with mother liquor were measured on a SIEMENS SMART CCD diffractometer, and the reflection data were collected at 293 K by ω scan technique using graphite-monochromated Mo Kα (λ = 0.71073 Å) radiation. The

Table 1. Crystallographic Data for Complexes **3**·1/2$C_2H_4Cl_2$, **5**·CH_2Cl_2·2CH_3OH, and **6**·2CH_2Cl_2·3/2CH_3OH·1/2H_2O

	3·1/2$C_2H_4Cl_2$	**5**·CH_2Cl_2·2CH_3OH	**6**·2CH_2Cl_2·1/2CH_3OH·3/2H_2O
empirical formula	$C_{34}H_{31}ClFeN_3P_2$	$C_{67}H_{68}Cl_2F_6Fe_2N_3O_2P_4Sb$	$C_{86.5}H_{79}Cl_4F_6N_3O_2P_4Ru_2Sb$
fw	634.86	1489.47	1896.10
space group	$P\bar{1}$	$P2_1/c$	$P\bar{1}$
a, Å	9.5782(3)	13.2975(2)	15.3230(5)
b, Å	11.0580(3)	18.5124(4)	15.4279(5)
c, Å	14.4083(4)	29.1127(4)	21.5190(7)
α, deg	88.529 (1)		84.380(1)
β, deg	82.181(1)	102.137(1)	82.280(1)
γ, deg	88.924(1)		65.179(1)
V, Å^3	1511.20(8)	7006.4(2)	4570.5(3)
Z	2	4	2
ρ_{calcd}, g/cm^3	1.395	1.412	1.378
μ, mm^{-1}	0.722	1.019	0.863
radiation (λ, Å)	0.71073	0.71073	0.71073
temp, K	293(2)	293(2)	293(2)
R1(F_o)[a]	0.0608	0.0946	0.0681
wR2(F_o^2)[b]	0.1396	0.2200	0.1885
GOF	1.157	1.133	1.177

[a] $R1 = \sum|F_o - F_c|/\sum F_o$. [b] $wR2 = \sum[w(F_o^2 - F_c^2)_2]/\sum[w(F_o^2)]^{1/2}$.

Table 2. Crystallographic Data for Complexes **7**, **8**·H_2O, and **9**

	7	**8**·H_2O	**9**
empirical formula	$C_{35}H_{29}C_{10}FeN_3P_2$	$C_{45}H_{37}N_3P_2Ru$	$C_{67}H_{58}F_3Fe_2N_3O_3P_4S$
fw	609.40	798.79	1277.8
space group	$P\bar{1}$	$P2_1/n$	$C2/c$
a, Å	9.5641(2)	10.5627(2)	16.4730(2)
b, Å	11.8008(1)	22.5231(1)	18.0376(3)
c, Å	14.2658(3)	17.3953(4)	20.8622 (1)
α, deg	82.780(1)		
β, deg	84.37	97.422(1)	93.348(1)
γ, deg	71.671(1)		
V, Å^3	1513.36(5)	4103.75(12)	6188.28(13)
Z	2	4	4
ρ_{calcd}, g/cm^3	1.337	1.293	1.372
μ, mm^{-1}	0.633	0.496	0.664
radiation (λ, Å)	0.71073	0.71073	0.71073
temp, K	293(2)	293(2)	293(2)
R1(F_o)[a]	0.0688	0.0677	0.0678
wR2(F_o^2)[b]	0.1460	0.1968	0.1569
GOF	1.113	1.234	1.122

[a] $R1 = \sum|F_o - F_c|/\sum F_o$. [b] $wR2 = \sum[w(F_o^2 - F_c^2)_2]/\sum[w(F_o^2)]^{1/2}$.

data intensity was corrected for LP factors, and the SADABS technique was applied for absorption corrections. The metal atoms were determined by Patterson procedure for **9** whereas by direct methods for other compounds. The remaining non-hydrogen atoms were located from the successive difference Fourier syntheses. The structures were refined on F^2 by full-matrix least-squares method using the SHELXTL-97 program package.[29] The non-hydrogen atoms were refined anisotropically whereas the hydrogen atoms were generated geometrically and refined with isotropic thermal parameters.

The refinements of **3**·1/2$C_2H_4Cl_2$, **5**·CH_2Cl_2·2CH_3OH, and **6**·2CH_2Cl_2·1/2CH_3OH·3/2H_2O were performed by fixing the C−Cl (1.760 ± 0.005 Å) and C−O (1.420 ± 0.005 Å) distances of the solvate 1,2-dichloroethane, dichloromethane, and methanol. The problem of crystal quality for **5**·CH_2Cl_2·2CH_3OH resulted in a relative high *R* factor (0.0946). For **6**·2CH_2Cl_2·1/2CH_3OH·3/2H_2O, the occupancy factors of atoms C03, Cl1, and Cl2 in the solvate dichloromethane are 0.50, respectively. For **7**, the carbon (C51, C52, C53, C54, C55, and C56) atoms in one of the phenyl groups were fixed as rigid bodies, with C−C distances of 1.390 Å. For **9**, the trifluoromethanesulfonate exhibits a statistical distribution with the occupancy factors of 0.50 for atoms S, C, O1, O2, O3, F1, F2, and F3, respectively.

Physical Measurements. Elemental analyses (C, H, N) were performed on a Perkin-Elmer model 240C automatic instrument. The electrospray mass spectra (ES-MS) were recorded on a Finngan LCQ mass spectrometer using dichloromethane−methanol as mobile phase. The UV−vis spectra in dichloromethane solutions were measured on a Perkin-Elmer Lambda 25 UV−vis spectrometer. IR spectra were recorded on a Magna750 FT-IR spectrophotometer with KBr pellet. ^1H and ^{31}P NMR measurements were made on a Bruker AM500 spectrometer with $SiMe_4$ as the internal reference and 85% H_3PO_4 as external standard, respectively. The cyclic voltammogram was obtained by use of a potentiostat/galvanostat model 263A in 1 mM dichloromethane solutions containing 0.1 M (Bu_4N)PF_6 as supporting electrolyte at a scan rate of 100 mV s^{-1}. Platinum and glassy graphite were used as working and counter electrodes, respectively, the potentials were referenced to Ag/AgCl, and under the present experimental conditions, the ferrocenium/ferrocene couple was observed at 0.585 V.

Results and Discussion

Dicyanamide/tricyanomethanide-containing mononuclear organometallic compounds were prepared in high yields by the reactions between chloride-containing compounds and excess sodium dicyanamide or potassium tricyanomethanide. The reactions of the dicyanamide/tricyanomethanide-containing mononuclear compounds with the chloride-containing organometallic components **1** or **2** in equimolar ratios led to the isolation of dicyanamide/tricyanomethanide-bridged binuclear complexes. The binuclear arrays of **5**, **6**, **9**, and **10** could also be accessible by the direct reactions between the chloride-containing mononuclear components (**1** or **2**) and sodium dicyanamide/potassium tricyanomethanide in 2:1 molar ratios. Nevertheless, attempts to isolate pure products of the heterobinuclear species [Cp(dppe)FeN(CN)$_2$RuCp(PPh$_3$)$_2$]$^+$ and [Cp(dppe)FeC(CN)$_3$RuCp(PPh$_3$)$_2$]$^+$ were unsuccessful by the combination of the dicyanamide- (**3** or **4**) or tricyanomethanide-containing (**7** or **8**) synthons with the chloride-containing components (**1** or **2**) because the products were contaminated by the impurity of the homobinuclear species which was extremely difficult to remove by crystallization as well as by chromatography.

The IR spectra of complexes **3**−**10** showed characteristic stretching vibration bands of dicyanamide and tricyanomethanide, respectively. Relative to ν(N(CN)$_2$) values of the free ligand (2287, 2229, and 2181 cm^{-1}), those of mononuclear compounds **3** (2266, 2224, and 2158 cm^{-1}) and **4** (2270, 2229, and 2164 cm^{-1}) indicated a lower frequency shift due to the σ donation from the ligand to the metal center upon coordination. The ν(N(CN)$_2$) values of the dicyanamide-bridged binuclear complexes **5** (2299 and 2208 cm^{-1}) and **6** (2295 and 2208 cm^{-1}), however, showed higher frequency shifts compared with those of mononuclear compounds **3** and **4**. Those shifts reflect the integrated electronic effect of σ donation from the bridging ligand to the organometallic centers as well as π back-donation from

(29) Sheldrick, G. M. *SHELXL-97, Program for the Refinement of Crystal Structures*; University of Göttingen: Göttingen, Germany, 1997.

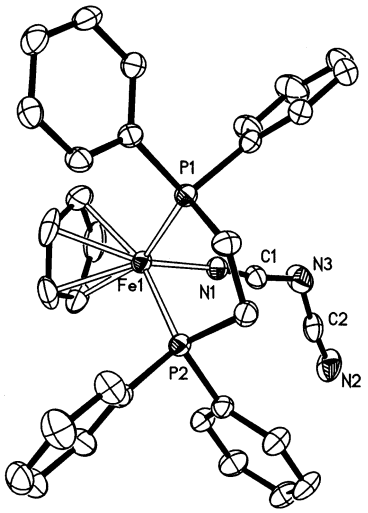

Figure 1. Perspective view of complex **3** with atom numbering scheme. Thermal ellipsoids are shown at the 30% probability level.

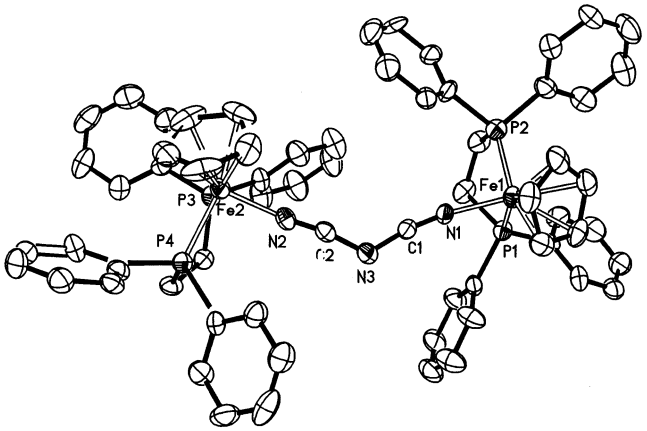

Figure 2. Perspective view of the complex cation of **5** with atom numbering scheme. Thermal ellipsoids are shown at the 30% probability level.

the organometallic center to the ligand. Upon one-electron oxidation, the IR spectra showed that the $\nu(N(CN)_2)$ of **5a** (2233, 2187, and 2087 cm^{-1}) exhibited significant shifts to low frequencies relative to those of its reduced form **5** (2299 and 2208 cm^{-1}). This shift reflects a great electronic flow that occurred from the bridging ligand to the metal centers upon oxidation. Compared with the $\nu(C(CN)_3)$ of the free ligand (2179s cm^{-1}), those of the mononuclear complexes **7** (2168s cm^{-1}) and **8** (2175s cm^{-1}) show a slight shift to lower frequencies. The $\nu(C(CN)_3)$ in the binuclear complexes **9** (2202m and 2185m cm^{-1}) and **10** (2201m and 2179s cm^{-1}) display a higher frequency shift relative to the mononuclear complexes **7** and **8**, reflecting the electronic effect from both σ donation and π back-bonding effects upon the formation of a bridging array.

The ORTEP plots of the dicyanamide-containing complexes **3**, **5**, and **6** are depicted in Figures 1, 2, and 3, respectively. Selected bond distances and angles of the three compounds are gathered in Table 3 for the purpose of comparison. In the terminal dicyanamide-bound complex **3**, the N−C bond distances (N1−C1= 1.138(5), C1−N3 = 1.311(6) Å) in the Fe-bonding end are the same as those in

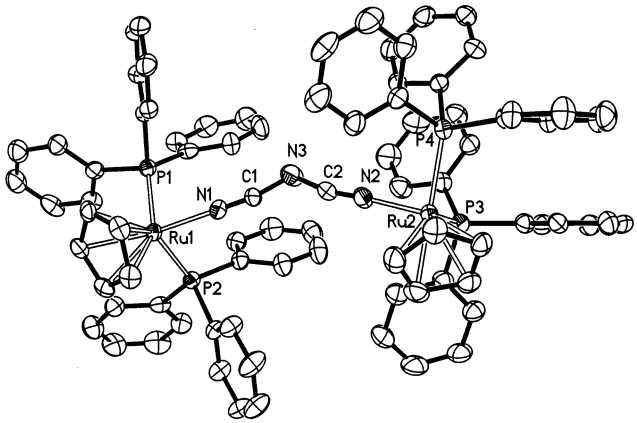

Figure 3. Perspective view of the complex cation of **6** with atom numbering scheme. Thermal ellipsoids are shown at the 30% probability level.

Table 3. Selected Bond Distances (Å) and Angles (deg) for Complexes **3**, **5**, and **6**

3		**5**		**6**	
Fe1−N1	1.928(4)	Fe1−N1	1.942(12)	Ru1−N1	2.073(7)
		Fe2−N2	1.945(13)	Ru2−N2	2.077(8)
Fe1−P1	2.2066(12)	Fe1−P1	2.218(4)	Ru1−P1	2.328(2)
Fe1−P2	2.2111(12)	Fe1−P2	2.187(5)	Ru1−P2	2.343(2)
		Fe2−P3	2.206(4)	Ru2−P3	2.330(2)
		Fe2−P4	2.213(4)	Ru2−P4	2.332(2)
Fe1−C51	2.088(5)	Fe1−C91	2.100(15)	Ru1−C131	2.226(9)
Fe1−C52	2.055(5)	Fe1−C92	2.090(15)	Ru1−C132	2.198(8)
Fe1−C53	2.061(5)	Fe1−C93	2.091(14)	Ru1−C133	2.186(8)
Fe1−C54	2.090(5)	Fe1−C94	2.082(15)	Ru1−C134	2.215(8)
Fe1−C55	2.086(5)	Fe1−C95	2.067(15)	Ru1−C135	2.236(8)
		Fe2−C96	2.083(17)	Ru2−C136	2.237(10)
		Fe2−C97	2.045(17)	Ru2−C137	2.233(10)
		Fe2−C98	2.077(18)	Ru2−C138	2.210(10)
		Fe2−C99	2.08(2)	Ru2−C139	2.198(9)
		Fe2−C100	2.102(17)	Ru2−C140	2.195(9)
N1−C1	1.138(5)	N1−C1	1.157(17)	N1−C1	1.129(10)
N2−C2	1.141(7)	N2−C2	1.136(17)	N2−C2	1.133(11)
N3−C1	1.311(6)	N3−C1	1.302(19)	N3−C1	1.311(13)
N3−C2	1.310(7)	N3−C2	1.299(19)	N3−C2	1.307(13)
N1−Fe1−P1	93.48(12)	N1−Fe1−P1	86.3(3)	N1−Ru1−P1	89.73(19)
N1−Fe1−P2	86.56(11)	N1−Fe1−P2	95.0(4)	N1−Ru1−P2	88.17(19)
P1−Fe1−P2	87.10(5)	P1−Fe1−P2	86.96(16)	P1−Ru1−P2	101.15(8)
		N2−Fe2−P3	87.4(3)	N2−Ru2−P3	88.4(2)
		N2−Fe2−P4	92.8(3)	N2−Ru2−P4	90.1(2)
		P3−Fe2−P4	86.66(15)	P3−Ru2−P4	101.25(8)
C1−N1−Fe1	171.3(4)	C1−N1−Fe1	168.7(12)	C1−N1−Ru1	174.2(7)
		C2−N2−Fe2	173.8(12)	C2−N2−Ru2	177.0(7)
N1−C1−N3	172.1(5)	N1−C1−N3	171.3(15)	N1−C1−N3	167.7(10)
C1−N3−C2	121.6(5)	C1−N3−C2	123.3(13)	C1−N3−C2	127.2(9)
N2−C2−N3	173.0(6)	N2−C2−N3	171.6(15)	N2−C2−N3	167.7(10)

the other end (N2−C2 = 1.141(7), C2−N3 = 1.310(7) Å). This phenomenon is more easily understood in complexes **5** and **6** once a symmetric bridging array M−NCNCN−M (M = Fe and Ru for **5** and **6**, respectively) is formed. Compared with the Fe−N, Fe−P, Fe−C, and C−N distances in mononuclear iron(II) compound **3**, those in the dicyanamide-bridged binuclear iron(II) complex **5** show simply a slight difference (Table 3). As depicted in Figures 2 and 3, the bridging array M−NCNCN−M (M = Fe and Ru for **5** and **6**, respectively) adopts a "V"-type conformation because of sp^2 hybridization of the middle nitrogen atom of the dicyanamide, where the C−N−C angle (123.3(13)° for **5** and 127.2(9)° for **6**) shows an appreciably larger deviation from 120° than that in mononuclear complex **3** (121.6(5)°).

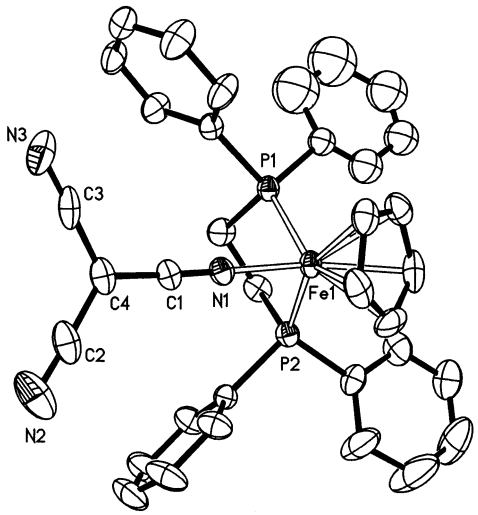

Figure 4. Perspective view of complex **7** with atom numbering scheme. Thermal ellipsoids are shown at the 30% probability level.

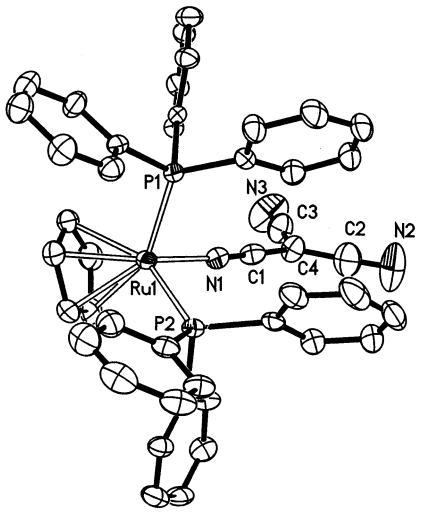

Figure 5. Perspective view of complex **8** with atom numbering scheme. Thermal ellipsoids are shown at the 30% probability level.

While the carbon atoms of the dicyanamide are sp hybridized, the N−C−N angles (167.7−172.1°) deviate moderately from linearity,[25,30] especially in dicyanamide-bridged binuclear ruthenium(II) complex **6** (167.7(10)°) which exhibits the most severe deviation among the three structurally characterized dicyanamide-containing complexes. The C−N−Fe angle is in the range 177.0(7)−168.7(12)°, deviating also from linearity. The metal···metal separations through a bridging dicyanamide are 8.088 and 8.501 Å, respectively, for complexes **5** and **6**.

The perspective views of tricyanomethanide-containing complexes **7**−**9** are shown in Figures 4−6, respectively. Selected bond distances and angles of the three compounds are gathered in Table 4 for the purpose of comparison. Relative to the Fe−N (1.921(4) Å) and Fe−P (average 2.221 Å) bond lengths of mononuclear complex **7** with terminal tricyanomethanide, those (Fe−N = 1.906(4) Å; av Fe−P = 2.201 Å) of tricyanomethanide-bridged binuclear complex

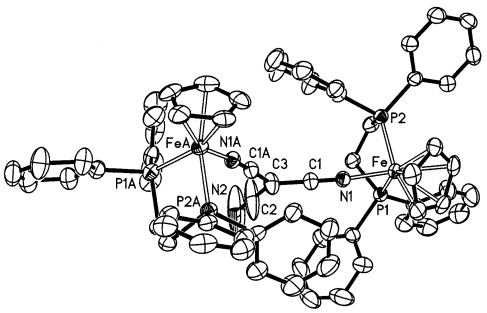

Figure 6. Perspective view of the complex cation of **9** with atom numbering scheme. Thermal ellipsoids are shown at the 30% probability level.

Table 4. Selected Bond Distances (Å) and Angles (deg) for Complexes **7**, **8**, and **9**

7		**8**		**9**	
Fe1−N1	1.921(4)	Ru1−N1	2.081(8)	Fe1−N1	1.906(4)
Fe1−P1	2.2234(15)	Ru1−P1	2.335(2)	Fe1−P1	2.2019(16)
Fe1−P2	2.2177(15)	Ru1−P2	2.325(2)	Fe1−P2	2.1994(15)
Fe1−C51	2.096(6)	Ru1−C71	2.188(9)	Fe1−C51	2.081(5)
Fe1−C52	2.067(6)	Ru1−C72	2.215(9)	Fe1−C52	2.084(6)
Fe1−C53	2.065(5)	Ru1−C73	2.223(10)	Fe1−C53	2.084(6)
Fe1−C54	2.088(6)	Ru1−C74	2.208(9)	Fe1−C54	2.078(6)
Fe1−C55	2.107(6)	Ru1−C75	2.184(9)	Fe1−C55	2.070(6)
N1−C1	1.154(6)	N1−C1	1.147(11)	N1−C1	1.148(6)
N2−C2	1.141(9)	N2−C2	1.155(16)	N2−C2	1.145(15)
N3−C3	1.143(9)	N3−C3	1.163(15)		
C1−C4	1.407(7)	C1−C4	1.378(15)	C1−C3	1.392(7)
C2−C4	1.426(9)	C2−C4	1.426(19)	C2−C3	1.403(14)
C3−C4	1.421(10)	C3−C4	1.424(18)		
N1−Fe1−P1	94.60(13)	N1−Ru1−P1	89.95(19)	N1−Fe1−P1	85.05(13)
N1−Fe1−P2	87.42(13)	N1−Ru1−P2	87.87(19)	N1−Fe1−P2	90.16(13)
P1−Fe1−P2	86.64(5)	P1−Ru1−P2	101.20(8)	P1−Fe1−P2	86.81(6)
C1−N1−Fe1	173.0(4)	C1−N1−Ru1	174.5(7)	C1−N1−Fe1	174.4(4)
N1−C1−C4	177.3(6)	N1−C1−C4	178.6(11)	N1−C1−C3	177.0(6)
N2−C2−C4	177.6(8)	N2−C2−C4	178.9(17)	N2−C2−C3	180.000(3)
N3−C3−C4	179.1(7)	N3−C3−C4	178.0(16)		
C1−C4−C2	120.9(6)	C1−C4−C2	121.1(10)	C1−C3−C2	119.4(4)
C1−C4−C3	119.4(5)	C1−C4−C3	119.1(10)	C1*−C3−C2	119.4(4)
C2−C4−C3	119.7(5)	C2−C4−C3	121.1(10)	C1−C3−C1*	121.3(7)

9 become shortened about 0.02 Å upon the formation of a bridging array $FeC(CN)_3Fe$, where the Fe−N−C angles (173.0(4)−174.4(4) Å) deviate appreciably from linearity. The tricyanomethanide is planar, and the sum of the bond angles (C−C−C) at the central carbon atom is equal to 360° because of the sp^2 hybridization.[31,32] The N−C−C angles (177.0(6)−180°) are close to 180° because of the sp hybridization of the cyano carbon atoms, in which the N−C and C−C distances are in the ranges 1.141−1.154 and 1.392−1.426 Å, respectively, showing a typical triple and conjugated single−double bonding character.[31,32] The Fe···Fe separation through a bridging tricyanomethanide is 7.883 Å, slightly shorter than that through a bridging dicyanamide observed in **5** (8.088 Å).

The redox chemistry of **3**−**10** was investigated by cyclic voltammetry, and the redox potentials are presented in Table 5. The mononuclear compounds **3**, **4**, **7**, and **8** afford a single reversible one-electron oxidation process, while the dicyanamide/tricyanomethanide-bridged binuclear complexes **5**,

(30) Jurgens, B.; Irran, E.; Schneider, J.; Schnik, W. *Inrog. Chem.* **2000**, *39*, 665.

(31) Dixon, D. A.; Calabrese, J. C.; Miller, J. S. *J. Am. Chem. Soc*. **1986**, *108*, 2582.

(32) Andersen, P.; Klewe, B.; Thom, E. *Acta Chem. Scand*. **1967**, *21*, 1530.

Table 5. Cyclic Voltammogram Data for Complexes **3**−**10**[a]

	$E_{1/2}$(ox1)/(ΔE_P)	$E_{1/2}$(ox2)/(ΔE_P)	$\Delta E_{1/2}$	K_c[b]
3	0.520(0.099)			
4	0.938(0.104)			
5	0.545(0.090)	0.686(0.081)	0.141	240
5a	0.563(0.062)	0.700(0.064)	0.137	210
6	0.922(0.113)	1.100(0.120)	0.178	1020
7	0.670(0.099)			
8	1.134(0.097)			
9	0.742(0.085)	0.915(0.082)	0.173	841
10	1.123(0.110)	1.365(0.102)	0.242	12333

[a] Potential data in volts vs Ag/AgCl are from single scan cyclic voltammograms recorded at 25 °C. Detailed experimental conditions are given in the Experimental Section. [b] The comproportionation constants, K_c, were calculated by the formula $K_c = \exp(\Delta E_{1/2}/25.69)$ at 298 K.

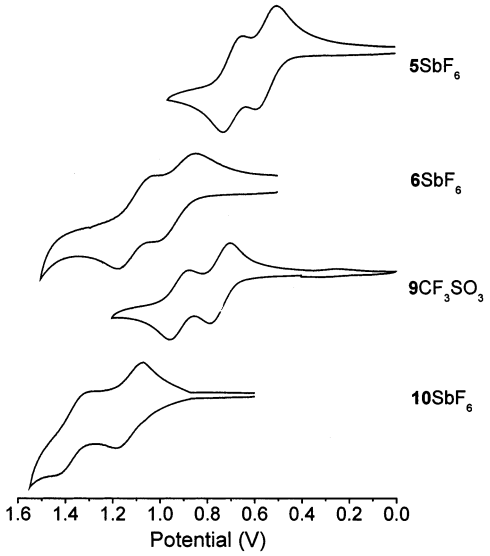

Figure 7. Cyclic voltammograms of dicyanamide-bridged dinuclear complexes **5** and **6** and tricyanomethanide-bridged complexes **9** and **10** recorded in 0.10 M dichloromethane solution of $(Bu_4N)PF_6$ at a scan rate of 0.10 V/s.

6, **9**, and **10** exhibit stepwise one-electron redox behavior (Figure 7). Obviously, an electronic coupling is operative between the redox termini through the bridging dicyanamide or tricyanomethanide. By comparison of the oxidation potential separation ($\Delta E_{1/2}$) between the two redox processes, it is observed that the electronic communications in the complexes **6** ($\Delta E_{1/2} = 0.178$ V) and **10** ($\Delta E_{1/2} = 0.242$ V) with $Cp(PPh_3)_2Ru$ as redox termini are appreciably greater, respectively, than those in the corresponding complexes **5** ($\Delta E_{1/2} = 0.141$ V) and **9** ($\Delta E_{1/2} = 0.173$ V) with Cp(dppe)-Fe as redox-active centers. This is easy to understand considering that ruthenium can afford a better π back-donation than iron to the bridging ligand. Moreover, the electron transfer mediated by bridging tricyanomethanide is more efficient relative to that by bridging dicyanamide[25] in view of the larger $\Delta E_{1/2}$ in the tricyanomethanide-bridged binuclear complexes **9** ($\Delta E_{1/2} = 0.173$ V) and **10** ($\Delta E_{1/2} = 0.242$ V) than those in the dicyanamide-bridged complexes **5** ($\Delta E_{1/2} = 0.141$ V) and **6** ($\Delta E_{1/2} = 0.178$ V). This phenomenon could be elucidated by the shorter MM distances through the bridging tricyanomethanide as well as the wider conjugate scale of the tricyanomethanide compared with the bridging dicyanamide.

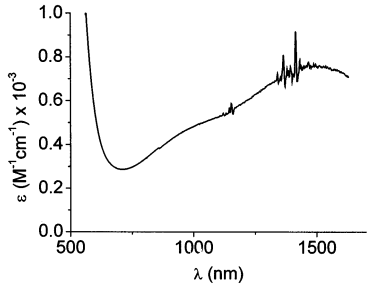

Figure 8. Near-infrared spectrum of **5a** in dichloromethane.

Mixed-valence compound **5a** was isolated as a stable solid species by the controlled oxidation of **5** with ferrocenium hexafluorophosphate in dichloromethane. The cyclic voltammogram showed it displays the same electrochemical behavior as its reduced form **5** affording two reversible one-electron redox couples (Table 5). In dichloromethane solution, **5a** exhibits a broad absorption band (Figure 8) in the near-infrared region centered at about 1500 nm ($\epsilon = 750$ cm^{-1} M^{-1}). The disappearance of such a band for **5** supports the assignment of this near-infrared band to intervalence charge transfer (IT) of the mixed-valence system in **5a**. Although further measurements of this intriguing IT band were hindered by the insufficient stability of **5a** in other organic solvents, application of Hush's theoretical analysis[33] of the IT band to **5a** is still possible. The half-width ($\Delta\nu_{1/2}$) is related to the energy of the IT band (ν_{max}) by the equation[34] $\nu_{max} - \nu_0 = (\Delta\nu_{1/2})^2/2310$, where ν_0 is the internal energy difference between **5** and **5a** with different oxidation states and can be estimated by the difference in the redox potential $\Delta E_{1/2}$. For **5a**, the difference in potentials from the cyclic voltamogram is 0.137 V which corresponds to $\nu_0 = 1100$ cm^{-1}. With the use of this equation, the calculated $(\Delta\nu_{1/2})_{calcd}$ is estimated to be 3580 cm^{-1}, while the corresponding observed $(\Delta\nu_{1/2})_{obsd}$ is 4850 cm^{-1}. Although the width of the intervalence band at half-height for the μ-dicyanamide molecule is somewhat greater than that calculated from Hush's equation derived for valence-trapped species, the ratio of 1.35 between the observed and calculated $\Delta\nu_{1/2}$ is typical for mixed-valence compounds of the class II type of the Robin and Day classification.[34−36] Another expression for the interaction parameter α^2 can be utilized to estimate the degree of ground-state delocalization in a mixed-valence complex, $\alpha^2 = 4.24 \times 10^{-4}[(\epsilon_{max}\Delta\nu_{1/2})/(\nu_{max}d^2)]$],[36] where d is the separation between two redox centers. Using the

(33) Hush, N. S. *Prog. Inorg. Chem.* **1967**, *8*, 391.
(34) (a) Dowling, N.; Henry, P. M.; Lewis, N. A.; Taube, H. *Inorg. Chem.* **1981**, *20*, 2345. (b) Colbran, S. B.; Robinson, B. H.; Simpson, J. *Organometallics* **1983**, *2*, 952. (c) Dowling, N.; Henry, P. M. *Inorg. Chem.* **1982**, *21*, 4088.
(35) Robin, M. B.; Day, P. *Adv. Inorg. Chem. Radiochem.* **1967**, *10*, 247.
(36) (a) Callahan, R. W.; Keene, F. R.; Meyer, T. J.; Salmon, D. J. *J. Am. Chem. Soc.* **1977**, *99*, 1064. (b) Colbert, M. C. B.; Lewis, J.; Long, N. J.; Raithby, P. R.; White, A. J. P.; Williams, D. J. *J. Chem. Soc., Dalton Trans.* **1997**, 99.

intramolecular Fe···Fe distance (8.1 Å) from the structural-analysis for **5**, a value for α^2 of 3.5×10^{-3} is calculated for mixed-valence complex **5a**. This value of α^2 is in the range calculated for Class II mixed-valence compounds.[6b,8d,35−37]

In 1982, Taube and co-workers[38] reported the electrochemical data and near-infrared spectra of the mixed-valence compound $[\{(NH_3)_5Ru\}_2N(CN)_2]^{5+}$, where it showed a small value of the comproportionation constant ($K_c = 340$) but a relatively large extinction coefficient ($\epsilon = 2800\ cm^{-1}\ M^{-1}$) for the intervalence band. Replacing trans ammonias by pyridine or by isonicotinamide decreases the electronic coupling ($K_c = 340-375$; $\epsilon = 2800-2310\ cm^{-1}\ M^{-1}$), revealing that the dominant coupling mechanism is πd(Ru)−π*(ligand) delocalization. In the dicyanamide-bridged organometallic compounds **5** and **6**, the comproportionation constants K_c are 240 and 1020 (Table 5), respectively. Relative to that observed in the dinuclear ruthenium complex $[\{NH_3)_5Ru\}_2N(CN)_2](PF_6)_2$ ($E_{1/2} = 0.149$ V, $K_c = 340$), the electronic coupling between two ruthenium centers through a bridging dicyanamide in the organometallic compound $[\{Cp(PPh_3)_2Ru\}_2N(CN)_2](SbF_6)$ (**6**) ($E_{1/2} = 0.178$ V, $K_c = 1020$) becomes stronger. Obviously, the electronic effect caused by the auxiliary ligands exerts an important role in the electronic delocalization of the dinuclear ruthenium compounds. In organometallic compound **6**, the PPh_3 and Cp ligands permit a higher degree of πd(Ru)−π*(N(CN)$_2$) back-bonding which results in a stronger electronic communication between the ruthenium centers through the dicyanamide bridge.

(37) Sutton, J. E.; Krentzien, H.; Taube, H. *Inorg. Chem.* **1982**, *21*, 2842.
(38) (a) Crutchley, R. J. *Adv. Inorg. Chem.* **1994**, *41*, 273. (b) Nelsen, S. F. *Chem. Eur. J.* **2000**, *6*, 581.

Conclusions

An efficient synthetic route is described for the preparation of dicyanamide/tricyanomethanide-bridged binuclear organometallic complexes by the incorporation between two metal components, one containing dicyanamide/tricyanomethanide with potential bridging group dicyanamide/tricyanomethanide, the other affording substitutable coordinated chloride. It has been demonstrated that the dicyanamide/tricyanomethanide could mediate an efficient electronic coupling between two organometallic redox termini with metal···metal separation more than 7.8 Å. The electronic coupling for the bridging array of tricyanomethanide is appreciably better than that for dicyanamide. The mixed-valence compound **5a**, belonging to a class II mixed-valence species, affords an intervalence transition band in the near-infrared region.

Acknowledgment. We are greatly grateful for the financial supports from NSF of China (20171044 and 20273074), the project for "hundred talents" from Chinese Academy of Sciences, and the startup foundation for scholars studying abroad from the ministry of education, China.

Supporting Information Available: X-ray crystallographic files in CIF format for the structure determinations of compounds **3** and **5**−**9**. This material is available free of charge via the Internet at http://pubs.acs.org.

IC025879T